Applied Surface Science 455 (2018) 70–74

Contents lists available at ScienceDirect

Applied Surface Science

journal homepage: www.elsevier.com/locate/apsusc

Full Length Article

# Control of $YH_3$ formation and stability via hydrogen surface adsorption and desorption

Olena Soroka[a,*], Jacobus M. Sturm[a], Robbert W.E. van de Kruijs[a], Chris J. Lee[b], Fred Bijkerk[a]

[a] Industrial Focus Group XUV Optics, MESA + Institute for Nanotechnology, University of Twente, Enschede, The Netherlands
[b] Institute of Engineering, Fontys Hogescholen, Eindhoven, The Netherlands

ARTICLE INFO

*Keywords:*
Hydrogenation
Atomic hydrogen
Yttrium hydride
Metal thin coatings
Surface desorption

ABSTRACT

Yttrium is known to form two hydrides: $YH_2$, a metal, and $YH_3$, which is dielectric. However, the stability of $YH_3$ is not fully understood, especially in the context of thin films, where the yttrium layer must be coated to protect it from oxidation. In this work, we show that the stability of a $YH_3$ thin film depends on the capping layer material. Our investigation reveals that $YH_3$ appears to be stabilized by hydrogen that is adsorbed to the capping layer surface. This is evidenced by the $YH_3$-$YH_2$ transition temperature, which was found to be correlated with the desorption temperature of hydrogen from the surface. We posit that surface-adsorbed hydrogen prevents hydrogen from diffusing out of the thin film, which limits $YH_3$ dissociation to the solubility of hydrogen in the $YH_2$/$YH_3$ thin film.

## 1. Introduction

The ability of rare-earth metals to form stable hydrides has found various applications in hydrogen storage, hydrogen sensing, and superconductivity. Yttrium is known to form di- and trihydrides, which was demonstrated in early works [1–4]. A pure bulk Y sample, exposed to ~1 bar of hydrogen and heated to 400 °C, reacts to form $YH_2$ [1]. $YH_3$ is formed once the temperature of $YH_2$ is lowered to 200 °C at a similar hydrogen pressure [2]. Further research showed that Y, in the form of a thin film (usually capped), does not powderize during hydrogenation, in contrast to bulk Y samples, allowing its electrical and optical properties to be extensively studied [5–9].

Later it was also found that a Y film, capped with a thin layer of Pd, simplifies the conditions needed for Y hydrogenation: hydride formation happens at lower hydrogen pressures and temperatures [7]. The role played by Pd is generally thought to be two-fold: (i) Pd dissociates $H_2$, providing a supply of reactive atomic hydrogen so that hydrogenation can proceed at room temperature, and (ii) Pd protects Y from oxidation, allowing hydrogenation. Interestingly, Pd capped Y hydrides are reversible at room temperature. Once the $H_2$ supply is removed, the $YH_3$ phase dissociates at room temperature to form $YH_2$ and $H_2$ [10]. According to Huiberts et al. [7], $YH_3$ stability in bulk is due to the bulk phase having a lower enthalpy of formation than a thin film. Furthermore, due to the unique catalytic properties of Pd, Y hydrogenation with other capping materials has not been studied.

In this paper, we present an investigation of the dependence between the stability of $YH_3$ and the capping layer material. We propose that the observed (measured) dissociation temperature of $YH_3$ is more properly associated with the desorption temperature of hydrogen from the surface of the capping layer. In our model, the dissociation temperature of $YH_3$ is lower than room temperature, however, if the hydrogen cannot escape from the surface, hydrogen diffusion is blocked and, thereby, the $YH_3$ phase is stabilized. As a result, $YH_3$ dissociation only occurs at temperatures above the $H_2$ surface desorption temperature of the capping layer.

## 2. Experimental procedure

All samples were deposited using DC magnetron sputtering. Sputter deposition took place in a vacuum chamber with a base pressure of $10^{-8}$ mbar using Y, Ru, Pd, and Ta targets with a purity of 99.95%, and Ag and C targets with purities of 99.99% and 99.999% respectively. Silicon (1 0 0) wafers, precut 15 × 15 mm, were coated with 70 nm of Y and then covered with a capping layer of Ru, Pd, Ag or Ta. To protect the cap metal from oxidation, 5 nm of carbon was sputtered onto the Ta and Ag capped samples, which was later removed by hydrogen radicals during the hydrogenation experiment.

After deposition, the thickness, roughness, and crystallinity of the deposited layers were measured using X-ray reflectivity (XRR), atomic force microscopy (AFM) (Bruker, Dimension Edge), and X-ray diffraction (XRD) (Panalytical Empyrean). XRD and XRR were performed using Cu Kα radiation with a wavelength of 0.154 nm. For XRD

* Corresponding author.
*E-mail address:* o.soroka@utwente.nl (O. Soroka).

https://doi.org/10.1016/j.apsusc.2018.05.134
Received 10 April 2018; Received in revised form 16 May 2018; Accepted 17 May 2018
Available online 24 May 2018
0169-4332/ 

measurements, a parafocusing geometry was chosen with a 0.2 mm fixed divergence slit and a Ni filter for the incident beam, and a scanning line detector to obtain a higher diffracted intensity and an increased signal to noise ratio. A cross-sectional analysis of a Ru capped Y sample was provided by a High Resolution Transmission Electron Microscope (Philips CM300ST-FEG Transmission Electron Microscope, MESA + Nanolab at University of Twente). TEM specimens were prepared by dimple grinding/polishing and argon ion etching [11].

Hydrogenation experiments were performed in a vacuum chamber with a base pressure of $1 \times 10^{-7}$ mbar and a hydrogen pressure of $1.3 \times 10^{-2}$ mbar. For all samples, a constant flow of hydrogen radicals was used. Hydrogen radicals were generated by flowing molecular hydrogen (108 sccm) past a W filament, placed about 5 cm from the sample surface, and heated to 2000 °C, as measured by an infrared temperature sensor (Raytek, RayMR1SCCF). Although Pd can dissociate molecular hydrogen, the $H_2$ splitting efficiency of a hot W filament is much higher, thus, hydrogenation occurs faster in the latter case. The hydrogen radical flux was estimated from the etch rate of a carbon film to be $10^{18}$ at/cm$^2$/s [12]. The sample temperature was monitored using a K-type thermocouple, and maintained at 30–40 °C by water cooling.

Hydrogenation of Y was monitored using *in situ* spectroscopic ellipsometry (Woollam M-2000XI) at an angle of incidence of 75° and a spectral range of 240–1600 nm. Exposure to H-radicals was stopped when the ellipsometric angles Ψ and Δ stabilized after a rapid change. The exposed samples were removed from the vacuum and tested with XRD, to characterize the hydride content.

Samples that formed a stable $YH_3$ phase after hydrogenation were heated in a nitrogen atmosphere on a hot stage of the Cu-K diffractometer and the dissociation temperature of $YH_3$ was measured. Heating was limited to temperatures below 350 °C, as heating to higher temperatures initiated oxidation of the Y film. The temperature was increased in 10 degree steps, and at each step XRD spectra were measured until no change in diffraction pattern was observed. The temperature at which the (0 0 2) peak of $YH_3$ started to decrease was noted as $YH_3$ dissociation temperature.

## 3. Results and discussions

### 3.1. Pre-characterization

The thicknesses of the Y films and capping layers were determined using XRR. Typical values are shown in Table 1. Overall, Y thickness for all samples was 70–80 nm and the thickness of single caps was 3–4 nm. Note, that the protective carbon layer on the Ag cap is significantly thinner than the targeted thickness, which may indicate the intermixing of Ag and C. In the case of the Pd/Ru cap, the thickness of Ru has to be increased to prevent the direct contact between Y and Pd. It is also important to note that fitting XRR spectra for Pd/Ru sample was challenging, because Ru and Pd have low contrast for hard X-rays.

The XRD spectra of all samples only contain peaks associated with the Y film (and Si substrate), as the peak intensity of the thin capping layer is negligibly small in θ-2θ geometry. The Y peaks of all as-deposited samples appear to be the same, therefore, only the XRD spectra of a Ru capped Y film is shown in Fig. 1. The vertical lines indicate tabulated Bragg peaks for powders. The peaks are shifted with respect to the tabulated values due to film stress. The small peak around 33°

**Table 1**
Thicknesses (in nm) of Y and capping layers for all sample types.

| Thicknesses | Caps | | | | |
|---|---|---|---|---|---|
| | Ta | Ru | Pd/Ru | Pd | Ag |
| Y | 73.6 | 72.4 | 79.7 | 72.3 | 70.2 |
| Cap | 3.8 | 2.9 | 4.4/5.4 | 4 | 3.4 |
| Carbon layer | 5 | – | – | – | 3.6 |

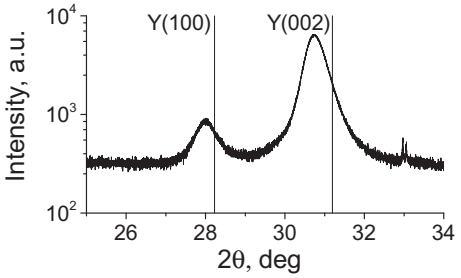


**Fig. 1.** XRD spectra of a typical as-deposited sample of 70 nm Y capped with 3 nm Ru.

originates from the Si monocrystalline substrate. It is observed that Y, grown on crystalline Si, is poly- or nanocrystalline with (0 0 2) and (1 0 0) preferential growth directions. The minimal crystallite size was estimated using the Scherrer relation [13]:

$$d = (0.94\lambda)/(w\cos\theta),$$

where $w$ is the full width at the half maximum of the XRD peak, λ – the radiation wavelength, and θ – the diffraction angle. The calculated Y crystallite size (in the direction normal to the sample surface) was estimated to be no less than 15 nm.

The surface of a typical sample is fairly smooth, as can be concluded from an AFM scan (Fig. 2), with root mean square roughness of 0.6 nm.

Bright field HRTEM images are shown in Fig. 3. The image shows that a thin amorphous intermixing layer is formed on the Ru/Y interface (visible by its brighter contrast compared to pure Ru, image 1). At the Y/Si interface, a 4 nm thick amorphous interface layer is formed (image 2). Its formation was probably induced by the reaction of Y with O that was contained in the native Si oxide layer, since Y oxide has a low enthalpy of formation. The orientation of the Y crystallites confirms the XRD findings, but the measured d-spacing of 3.06 Å indicates that the Y film is fully oxidized in the process of TEM specimen transfer and preparation.

### 3.2. Results

Samples were exposed to hydrogen radicals until no further change in ellipsometric angles Ψ and Δ were observed. Fig. 4 shows the time evolution of the ellipsometric angle Ψ at a wavelength of 791 nm during hydrogenation for samples with different capping layers. Depending on the sample, the following features are observed. For Ta and Ag capped samples, Ψ first increases as the carbon layer is removed by $H^*$. Likewise, for samples with Ru and Pd top surfaces, the first Ψ changes (a decrease in this case) are due to the removal of the native

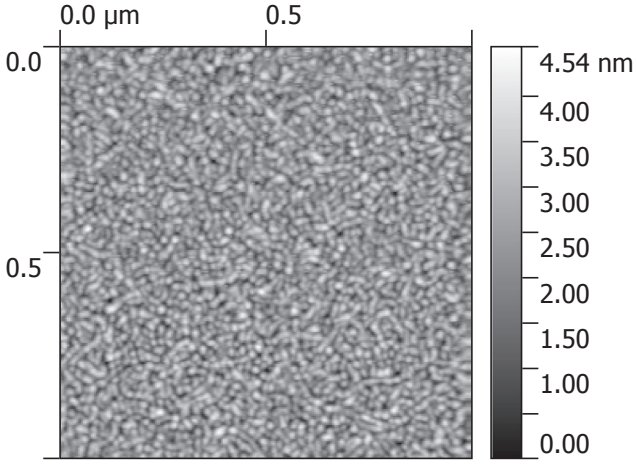


**Fig. 2.** AFM picture of the surface of a 3 nm Ru/70 nm Y sample.

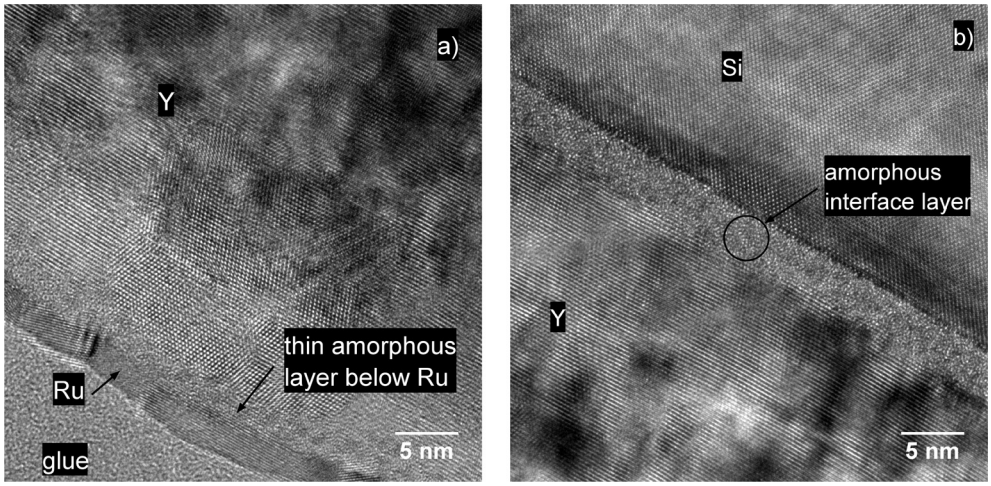


**Fig. 3.** HRTEM of 3Ru/70Y: (a) Ru/Y interface, (b) Y/Si interface.

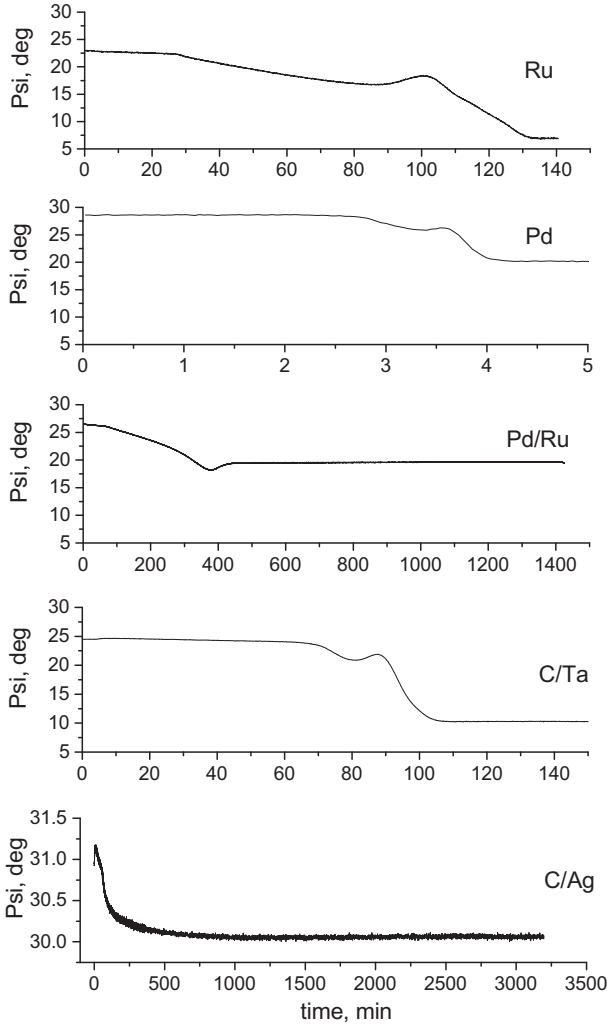


**Fig. 4.** Time evolution of ellipsometric angle Ψ for all samples at a wavelength of 791 nm during exposure to hydrogen radicals. The name of the capping material is indicated on each graph (note that the large difference in Ψ-axis scale for Ag capped sample). The W filament was switched on at time 0 and remained on till the end of the measurements shown on the figure.

oxide layer. After the removal of the protective coating, H may diffuse through the capping layer to reach the Y film and the formation of $YH_2$ starts, which may then be followed by the formation of $YH_3$. The transitions for Ru and Ta caps show similar dynamics, while almost no change in Ψ for samples with a Ag cap could be detected after a long exposure to $H^*$ (see Fig. 4).

After no change in the SE signal was registered, which suggests that the Y film is saturated with hydrogen, samples were transferred to the Cu-K diffractometer and their XRD spectra were measured under ambient conditions (Fig. 5). The diffraction patterns for both the Ru and Ta

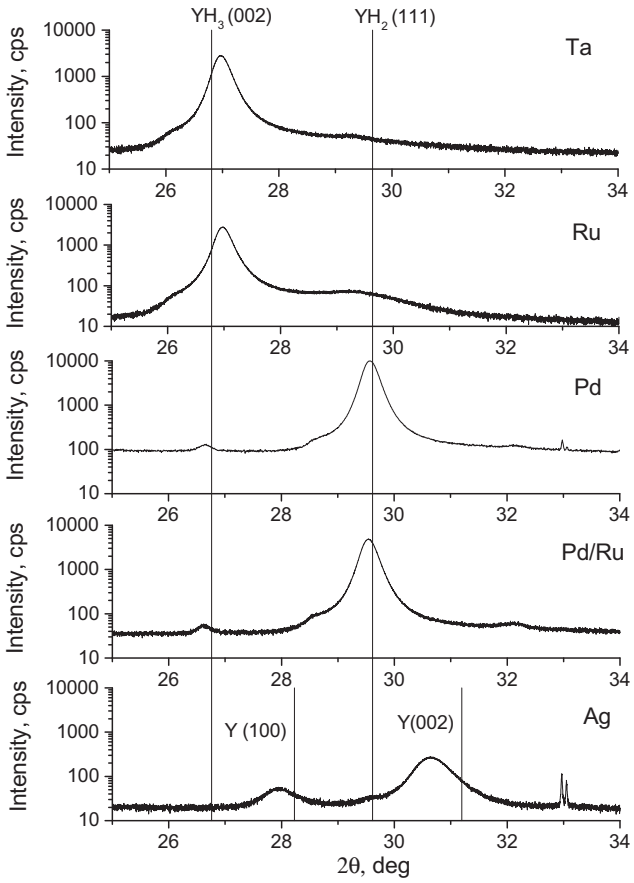


**Fig. 5.** XRD spectra of hydrogenated samples with different capping layers. The lines indicate the tabulated peaks for powders.

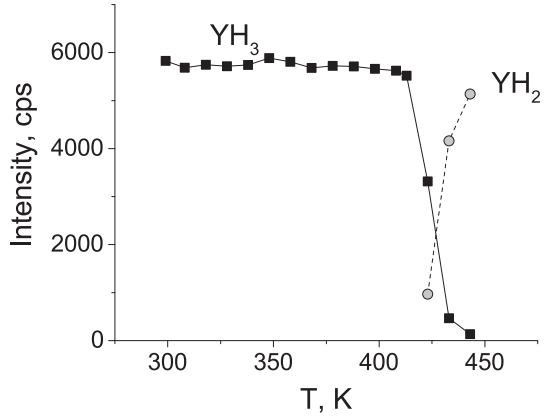


**Fig. 6.** Intensity of the diffraction peak (0 0 2) of $YH_3$ and (1 1 1) of $YH_2$ for a Ru/Y sample versus the temperature.

**Table 2**
Desorption temperatures of hydrogen for capping materials and dominant yttrium hydride phase of the corresponding hydrogenated sample.

| | Ta | Ru | Pd/Ru | Pd | Ag |
|---|---|---|---|---|---|
| $YH_x$ of saturated sample | $YH_3$ | $YH_3$ | $YH_2$ | | No hydride |
| Hydrogen desorption temperature of topmost capping layer, K | 775[a] | 410[b] | 293 (weakly bounded H)[c] | | 160[d] |

[a] Ref. [15].
[b] Ref. [14].
[c] Ref. [16].
[d] Ref. [17].

capped samples contain diffraction peaks of both a dominant $YH_3$ (0 0 2) phase, and a weak $YH_2$ (1 1 1) phase. On the other hand, the samples with Pd and Pd/Ru caps have a strong $YH_2$ peak along with some traces of a $YH_3$ (0 0 2) peak. The sample with Ag cap remains unchanged (comparing to before exposure, Fig. 1) except of the shoulder of the Y (0 0 2) peak, which may indicate that a minor amount of $YH_2$ is formed.

The growth of the $YH_3$ crystallite size for Ru capped samples was investigated in more detail. According the Scherrer equation, the $YH_3$ crystallite size was 33.2 nm, which is more than twice the deposited Y film crystallite size. This change in crystallite size is not due to lattice expansion after incorporating hydrogen, as the increase of the unit cell volume due to hydrogenation is only 12%. The increase in unit cell volume, however, closely matches XRR measurements, which show that the thickness of the Y film increases by 15% after hydrogenation. The growth of the crystallites is, thus, much larger than the film thickness growth, which evidences that hydrogenation leads to ordering of crystallites. Notably, the same rearrangement of crystallites in the Y film is observed for all types of samples where saturation to $YH_2$ or $YH_3$ phase was possible. This suggests that crystallite ordering already happens during the Y-$YH_2$ transition.

The $YH_3$ dissociation temperature was measured by heating the samples and measuring the changes in the XRD pattern. It was observed that $YH_3$ in Ru capped samples dissociated at 423 K, while, for Ta, the $YH_3$ dissociation temperature was above the maximum that could be achieved in our experimental apparatus. For Ag and Pd capped samples, $YH_3$ was not stable at room temperature, which was the minimum our setup was capable of. The intensity of the $YH_2$ (1 1 1) and $YH_3$ (0 0 2) peaks as a function of temperature is shown in Fig. 6 for the case of a Ru cap. The hydrogen desorption temperature for the Ru surface [14] is close to the dissociation temperature of $YH_3$ that we obtained, while the desorption temperature for Ta is much higher than the temperature limit of the setup (see Table 2).

## 4. Summary and conclusions

In this work, we studied the hydrogenation of thin Y films, coated with different materials. In the case of a Ag capping layer, no significant hydrogenation was observed. This may be due to the high desorption rate of hydrogen from the Ag surface at room temperature. For other samples the stable Y hydride phase was analyzed. For both Pd and Pd/Ru caps, the thermodynamically favorable $YH_2$ phase was formed, while a stable $YH_3$ phase was obtained for the cases of Ru and Ta caps. The samples with a $YH_3$ phase that was stable at room temperature were heated in an $N_2$ atmosphere to measure the temperature of $YH_3$ dissociation. The dissociation temperature for the Ru/$YH_3$ sample was 423 K, while the dissociation of $YH_3$ was not reached for the Ta capped sample due to the limited maximum temperature of the experimental setup ($T_{max}$ = 623 K). We note that the measured dissociation temperature for Ru/$YH_3$ is close to the reported temperature of hydrogen desorption from a Ru surface. We also noted that the desorption of hydrogen from Ta is reported to occur at 775 K [15], which is higher than the experimental setup allowed.

The formation (or lack of formation) of $YH_3$, depending on the cap layer provides reasonable evidence that the observed dissociation temperature of $YH_3$ is actually controlled by desorption of hydrogen from the capping layer surface. This evidence is strengthened by the observation that Pd-capped Ru/Y does not have a stable $YH_3$ phase at room temperature. If the direct interaction between the $YH_x$ phase and the cap-layer were the (de-)stabilizing factor, then Ru should stabilize $YH_3$ even when the Ru is capped with Pd. On the other hand, if $YH_3$ thin films are unstable at (or below) room temperature, then a stable $YH_3$ phase should not be observed in any of the samples.

During $YH_3$ dissociation, hydrogen will leave the thin film via diffusion from the surface. At equilibrium, the flux of hydrogen exiting the thin film will balance hydrogen production via dissociation. However, if hydrogen binds to the capping layer surface, the net flux will drop to zero. In this case, $YH_3$ dissociation will form an equilibrium with the hydrogen dissolved (or trapped) in the surrounding material ($YH_x$ and capping material). The small volume of dissolved hydrogen in the capping material and the low solubility of hydrogen in $YH_x$ imply that the majority of hydrogen must remain bound to Y to form $YH_3$. As a result, we conclude that the apparent stability or instability of $YH_3$ is, in case of thin films, governed by the surface desorption temperature of the capping layer.

## Note

Declarations of interest: none.

## Acknowledgments

The authors would like to thank Mr. Goran Milinkovic and Mr. John de Kuster for the technical support, and Mr. Theo van Oijen for deposition of samples. This work is part of the research programme of the Netherlands Organization for Scientific Research (NWO), Domain Applied and Engineering Sciences (AES, previously Technology Foundation STW). The work is additionally supported by ZEISS. We also acknowledge the support of the Industrial Focus Group XUV Optics at the MESA+ Institute at the University of Twente, notably the industrial partners ASML, ZEISS, Malvern Panalytical, and the Province of Overijssel.

## References

[1] H.E. Flotow, D.W. Osborne, K. Otto, Heat capacities and thermodynamic functions of $YH_2$ and $YD_2$ from 5° to 350°K and the hydrogen vibration frequencies, J. Chem. Phys. 36 (1962) 866–872, http://dx.doi.org/10.1063/1.1732681.
[2] H.E. Flotow, D.W. Osborne, K. Otto, B.M. Abraham, YH3and YD3: heat capacities and thermodynamic functions from 15° to 350°K and infrared absorption spectra, J. Chem. Phys. 38 (1963) 2620–2626, http://dx.doi.org/10.1063/1.1733561.

[3] A. Pebler, W.E. Wallace, Crystal structures of some lanthanide hydrides, J. Phys. Chem. 66 (1962) 148–151, http://dx.doi.org/10.1021/j100807a033.
[4] C.E. Lundin, J.P. Blackledge, Pressure-temperature-composition relationships of the yttrium-hydrogen system, J. Electrochem. Soc. 109 (1963) 838–842.
[5] A.E. Curzon, O. Singh, Thin film studies of yttrium, yttrium hydrides and yttrium oxide, J. Phys. F Met. Phys. 8 (1978) 1619–1625, http://dx.doi.org/10.1088/0305-4608/8/8/003.
[6] D.J. Santjojo, T. Aizawa, S. Muraishi, Ellipsometric characterization on multi-layered thin film systems during hydrogenation, Mater. Trans. 48 (2007) 1380–1386, http://dx.doi.org/10.2320/matertrans.MRA2006193.
[7] J.N. Huiberts, R. Griessen, J.H. Rector, R.J. Wijngaarden, J.P. Dekker, D.G. de Groot, N.J. Koeman, Yttrium and lanthanum hydride films with switchable optical properties, Nature 380 (1996) 231–234, http://dx.doi.org/10.1038/380231a0.
[8] N. Strohfeldt, A. Tittl, M. Schäferling, F. Neubrech, U. Kreibig, R. Griessen, H. Giessen, Yttrium hydride nanoantennas for active plasmonics, Nano Lett. 14 (2014) 1140–1147, http://dx.doi.org/10.1021/nl403643v.
[9] P. Ngene, T. Radeva, M. Slaman, R.J. Westerwaal, H. Schreuders, B. Dam, Seeing hydrogen in colors: low-cost and highly sensitive eye readable hydrogen detectors, Adv. Funct. Mater. 24 (2014) 2374–2382, http://dx.doi.org/10.1002/adfm.201303065.
[10] E.S. Kooij, A.T.M. Van Gogh, D.G. Nagengast, N.J. Koeman, R. Griessen, Hysteresis and the single-phase metal-insulator transition in switchable YHx films, Phys. Rev. B – Condens. Matter Mater. Phys. 62 (2000) 10088–10100, http://dx.doi.org/10.1103/PhysRevB.62.10088.
[11] E.G. Keim, M.D. Bijker, J.C. Lodder, Preparation of cross-sectional transmission electron microscopy specimens of obliquely deposited magnetic thin films on a flexible tape, J. Vac. Sci. Technol. A Vacuum, Surfaces, Film 19 (2001) 1191–1194, http://dx.doi.org/10.1116/1.1330259.
[12] O.V. Braginsky, A.S. Kovalev, D.V. Lopaev, E.M. Malykhin, T.V. Rakhimova, A.T. Rakhimov, A.N. Vasilieva, S.M. Zyryanov, K.N. Koshelev, V.M. Krivtsun, M. van Kaampen, D. Glushkov, Removal of amorphous C and Sn on Mo: Si multi-layer mirror surface in Hydrogen plasma and afterglow, J. Appl. Phys. 111 (2012) 93304, http://dx.doi.org/10.1063/1.4709408.
[13] A.L. Patterson, The Scherrer formula for X-ray particle size determination, Phys. Rev. 56 (1939) 978–982, http://dx.doi.org/10.1103/PhysRev. 56.978.
[14] K.L. Kostov, W. Widdra, D. Menzel, Hydrogen on Ru (001) revisited: vibrational structure, adsorption states, and lateral coupling, Surf. Sci. 560 (2004) 130–144, http://dx.doi.org/10.1016/j.susc.2004.04.025.
[15] D.E. Shleifman, D. Shaltiel, I.T. Steinberger, Thermally stimulated hydrogen desorption from zirconium and tantalum, J. Alloys Compd. 223 (1995) 81–86, http://dx.doi.org/10.1016/0925-8388(94)01497-3.
[16] J.A. Konvalinka, J.J.F. Scholten, Sorption and temperature-programmed desorption of hydrogen from palladium and from palladium on activated carbon, J. Catal. 48 (1977) 374–385, http://dx.doi.org/10.1016/0021-9517(77)90111-7.
[17] R. Duś, E. Nowicka, Atomic deuterium (hydrogen) adsorption on thin silver films, Prog. Surf. Sci. 74 (2003) 39–56, http://dx.doi.org/10.1016/j.progsurf.2003.08.004.